A NOVEL QUASI-ELLIPTIC WAVEGUIDE TRANSMIT REJECT FILTER FOR KU-BAND VSAT TRANSCEIVERS

Z.-B. Xu[*], J. Guo, C. Qian, and W.-B. Dou

State Key Laboratory of Millimeter Waves, Southeast University, Nanjing 210096, China

Abstract—In this paper, a novel compact quasi-elliptic waveguide low-pass transmit reject filter (TRF) by using T-shape units is proposed for Ku-band very small aperture terminal (VSAT) transceivers. The equivalent circuit model of the T-shape unit is investigated and shows a topology similar to that of the elliptic low-pass filter. In order to reduce the difficulty in physical realization, which is commonly encountered with a standard elliptic low-pass filter, an approximate elliptic low-pass filter prototype is presented. Accordingly, a synthesis approach is developed to obtain the initial dimensions of the filter. To optimize the performance of the filter, full-wave electromagnetic simulation is used to fine-tune the dimensions of the filter. An eleven-order Ku-band low-pass TRF is designed and fabricated using a WR-75 waveguide. Measured results show it has a low insertion loss of less than $0.3\,\text{dB}$ in the pass band and a high attenuation slope of $78\,\text{dB/GHz}$. Moreover, the miniaturized size of the filter is only $38\,\text{mm} \times 38\,\text{mm} \times 42\,\text{mm}$ (WR-75 flange size is $38\,\text{mm} \times 38\,\text{mm}$).

1. INTRODUCTION

In recent decades, very small aperture terminal (VSAT) networks have spread throughout the world. The demand for small VSAT transceivers has increased because of their portability, low cost and high reliability. Since the transceiver contains both transmitter and receiver, a transmit reject filter (TRF) unit is required to reject transmitting signal and noise leakage from the transmitter, which can

adversely affect the operation of the low noise amplifier in the low noise block (LNB). Typical receiving frequency band and transmitting frequency band of Ku-band VSAT station are 10.7–12.75 GHz and 14–14.5 GHz, respectively [1]. The gap between the two frequency bands is very small, thus a high out-of-band rejection TRF with sharp-skirt characteristic is indispensable in order to effectively attenuate leakage transmit signal. Furthermore, a low insertion loss in the pass band of the TRF is required for reducing the noise level of the receiver.

Since the TRF requires a low insertion loss, this means microstrip line filters [2–9] cannot meet this requirement. Low-pass filters with defected ground structure (DGS) [10–15] have been received increased attention in recent years for their unique features such as sharp cut-off frequency response, compact size and good performance in both the pass band and the stop band. However, their insertion loss is also too high for them being used as TRFs. Many types of waveguide filters can be used as TRFs [16–20]. Those filters have very low insertion loss in the pass band and high attenuation in the stop band, but bulky structure makes them unsuitable for compact transceivers, especially when the block of up converter (BUC), LNB, ortho-mode transducer (OMT) and TRF units are integrated in a small sealed housing. Dielectric- filled rectangular waveguide filters [21] dramatically reduced the size of the conventional air filled rectangular waveguide filters. However, their insertion loss is increased due to the dielectric loss. Substrate-integrated waveguide (SIW) filters [22–29] show a compact size, but high insertion loss prohibits them from being used as TRFs. Elliptic function filters [30] have very good selectivity performance, but they are hard to physically realize with the rectangular waveguide.

A miniaturized waveguide low-pass filter with an elliptic function response for Ku-band VSAT transceiver is presented in this paper, as shown in Fig. 1. The equivalent-circuit model for the T-shape unit is developed. Then, a quasi-elliptic low-pass filter prototype network, which is much easier in the physical realization is proposed to synthesize the dimensions of the filter. After the initial dimensions of the filter are obtained, CST Design Environment is used to optimize the performance of the filter. The design method and proposed filter are validated by achieving a good agreement between experiment and simulation. Both simulated and experimental results show that the proposed TRF achieves a very sharp cut-off response with a low insertion loss. Meanwhile, the designed TRF shows a compact size of 38 mm × 38 mm × 42 mm including the size of the waveguide flanges.
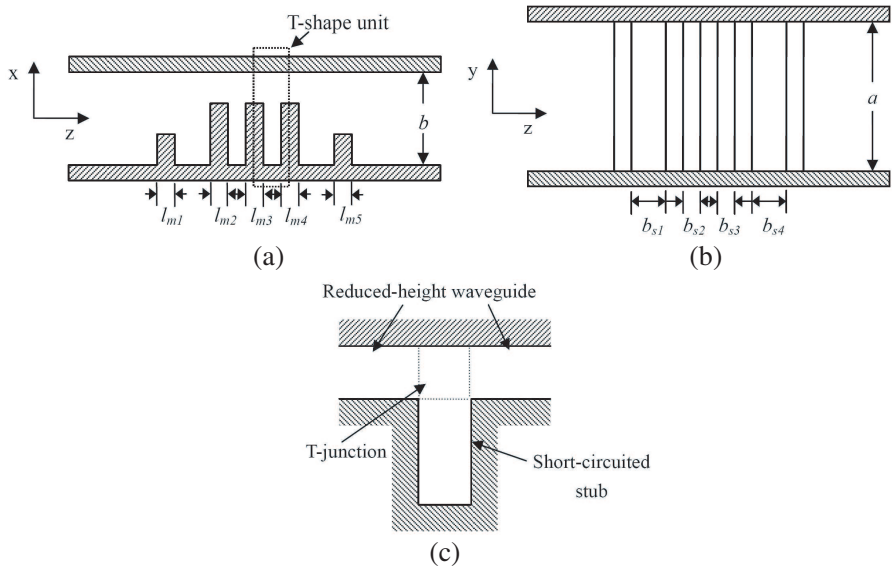
Figure 1. Structure of the proposed low-pass filter. (a) Side view. (b) Top view. (c) T-shape unit.

2. EQUIVALENT CIRCUIT FOR THE T-SHAPE UNIT

The T-shape unit can be modeled as an open E-plane T-junction with a series short-circuited stub and main waveguide with reduced height in its cross section, as shown in Fig. 1(c). The equivalent circuit of the T-junction can be obtained from [31], as illustrated in Fig. 2(a), where Z_m and Z_s is the normalized characteristic impedance of the reduced height waveguide and short-circuited stub, respectively. The value of d_m and $l_{s'}$ can be obtained from [31], then the susceptance looking forward to the short-circuited stub from the reference plane T' can be achieved by the following expression

$$jB_s = -j\frac{1}{m^2 Z_s}\cot(\beta l) \tag{1}$$

where, m is the transformer ratio for open E-plane T-junction defined by N. Marcuvitz in [31], β is the phase constant of the short-circuited stub waveguide, $l = l_s + l_{s'}$ is the effective length of the short-circuited stub waveguide. Accordingly, the total series susceptance caused by the short-circuited stub and T-junction is the sum of the Y and Y_s. By selecting l_s to satisfy $Y_s = -Y$, a parallel resonator can be obtained. Therefore, the open E-plane T-junction with the series short-circuited
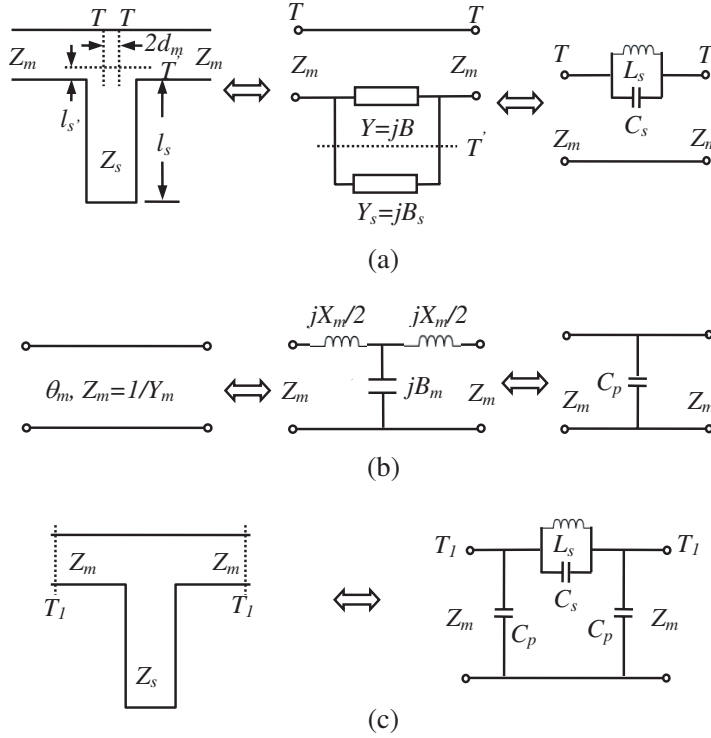
Figure 2. Equivalent circuit of: (a) T-junction with a short-circuited stub. (b) Reduced-height waveguide. (c) T-shape unit.

stub can be modeled as an equivalent L-C parallel resonator, as shown in Fig. 2(a). By forcing them to have the same resonant frequency f_0 and same susceptance at the cutoff frequency f_c ($f_c < f_0$) of the filter, the equivalent L_s and C_s can be extracted as

$$C_s = \frac{1}{Z_0} \frac{\omega_c}{\omega_0^2 - \omega_c^2} \left[\frac{Y_s}{m^2} \cot\left(\frac{\pi}{2} \frac{\lambda_{g0}}{\lambda_{gc}}\right) - B \right] \tag{2}$$

$$L_s = \frac{1}{\omega_0^2 C_s} \tag{3}$$

where Z_0 is the reference impedance of the filter, ω_0 and ω_c are the angular frequency corresponding to f_0 and f_c, respectively, $Y_s = 1/Z_s$ is the normalized characteristic admittance of the short-circuited stub, λ_{g0} and λ_{gc} is the operating wavelength of the short-circuited stub at the frequency f_0 and f_c, respectively.

The short length of a waveguide with reduced height can be served

as a T-network as illustrated in Fig. 2(b). By imposing them to the same ABCD matrix, $X_m/2$ and B_m can be derived as follows.

$$\frac{X_m}{2} = Z_m \tan \theta_m \tag{4}$$

$$B_m = Y_m \sin \theta_m \tag{5}$$

where Y_m and θ_m are the normalized admittance and electrical length of the height-reduced waveguide, respectively. If $Z_m \ll 1$ and $\theta_m < \pi/4$, the inductance of the T-network can be neglected and the short height-reduced waveguide is simplified as a shunt capacitance, as shown in Fig. 2(b). The equivalent shunt capacitance is found to be

$$C_p = \frac{1}{Z_0} \frac{Y_m \sin \left(\frac{2\pi}{\lambda_{gc}} l_m \right)}{\omega_c} \tag{6}$$

where l_m is the length of the height-reduced waveguide.

With the equivalent circuits mentioned above, the whole equivalent model of the T-shape unit can be represented by a lump L-C network, as shown in Fig. 2(c). Observing the equivalent circuit, it shows a topology similar to that of an elliptic low-pass filter. Therefore, the circuit shown in Fig. 2(c) should give an elliptic low-pass response by selecting each parameter properly.

The asymmetrical T-shape unit can be approximated as a symmetrical unit with a step in the E-plane, as shown in Fig. 3. Considering the effect introduced by the step, an extra capacitance C_{ps} is added in shunt configuration, as shown in Fig. 3.

In order to verify the equivalent circuit discussed above, a low-pass filter using a T-shape unit with a direct-coupled input and output rectangular waveguide is investigated. The physical structure and equivalent circuit of the filter are shown in Fig. 4. The dimensions of filter are optimized by using CST Design Environment and obtained as $a = 19.05 \, \text{mm}$, $b = 9.525 \, \text{mm}$, $b_m = 4 \, \text{mm}$, $b_s = 3 \, \text{mm}$, $l_m = 1.5 \, \text{mm}$, and $l_s = 8.525 \, \text{mm}$. Accordingly, the equivalent L-C values can be found from (2)–(6). The value of the C_{ps} can be obtained from [31]. The calculated equivalent L-C values are $C_{ps} = 0.0133 \, \text{pF}$,
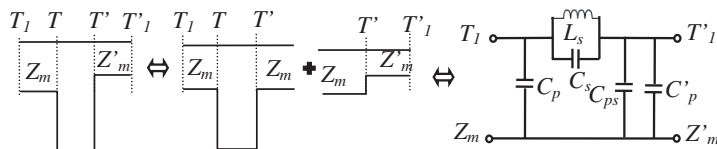

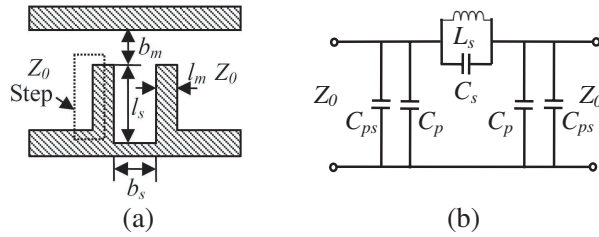**Figure 3.** Equivalent circuit of asymmetrical T-shape unit.

Figure 4. Low-pass filter using one T-shape unit. (a) Physical structure. (b) Equivalent circuit.
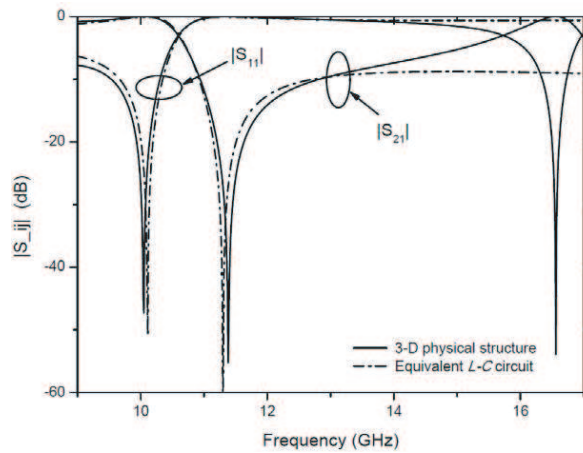

Figure 5. Simulated frequency response of the filter using one T-shape unit.

$C_p = 0.0271\,\text{pF}$, $L_s = 1.45\,\text{nH}$, and $C_s = 0.137\,\text{pF}$, respectively. The reference impedance of the filter is chosen to be $Z_0 = 470\,\text{Ohms}$, which is the wave impedance at 13 GHz inside the waveguide. The equivalent $L\text{-}C$ circuit is simulated using Agilent ADS. Fig. 5 shows the simulation results of the filter using both the equivalent $L\text{-}C$ circuit and 3-D physical structure. As shown in Fig. 5, an elliptic low-pass response is observed. The two simulation results are in very good agreement within the pass band and lower stop band of the filter. Due to the impact of the higher-order modes in the waveguide, a second harmonic resonant frequency is observed in the 3-D physical structure based simulation result, which may cause a deviation from the equivalent $L\text{-}C$ circuit based simulation result.

3. PROTOTYPE AND SYNTHESIZED METHOD

It is hard to synthesize a rectangular waveguide low-pass filter using the standard elliptic function element-value [32]. This is due to the fact that inductances and capacitances between the resonators show a high variation, which results in a difficulty in its physical realization. To obtain a proper prototype network, which is suitable for the rectangular waveguide realization and retain the elliptic function response at the same time, an approximate quasi-elliptic low-pass filter prototype network is proposed. The proposed network is derived from the Chebyshev response filter by replacing the inductance with a proper parallel resonator, as shown in Fig. 6. The element value of the Chebyshev response network can be obtained by using the available Chebyshev function table with proper impedance and frequency scaling. Choosing the resonant frequency of the parallel resonator properly at the stop band of the filter and equalizing the susceptance of the parallel resonator to $1/j\omega L_{sc}$ at the cut-off frequency of the filter, L_s and C_s of the resonator can be obtained. By setting the value of C_{pi} equal to that of C_{pci} ($i = 1, 2, 3 \ldots$), the initial values of the proposed quasi-elliptic filter prototype network are determined. Then, by using the circuit simulator, such as Agilent ADS, optimized L-C values of the proposed prototype network can be obtained.

The physical dimensions of the filter can be synthesized by using the L-C values of the proposed elliptic low-pass filter net-work. The normalized characteristic admittance of the short-circuited stub can be
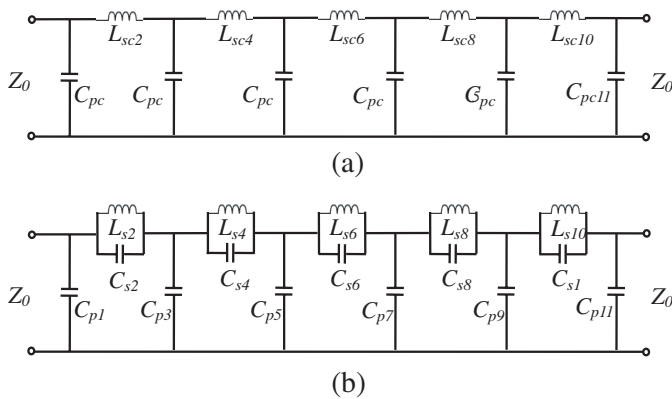

(a)

(b)

Figure 6. Chebyshev function low-pass filter net-work and proposed elliptic low-pass filter net-work.

transformed from (2).

$$Y_s = m^2 \left[C_s Z_0 \frac{\omega_0^2 - \omega_c^2}{\omega_c} + B \right] \tan \left(\frac{\pi}{2} \frac{\lambda_{g0}}{\lambda_{gc}} \right) \qquad (7)$$

As $Y_s = b/b_s$, b_s can be calculated as follow

$$b_s = \frac{b}{m^2 \left[C_s Z_0 \frac{\omega_0^2 - \omega_c^2}{\omega_c} + B \right] \tan \left(\frac{\pi}{2} \frac{\lambda_{g0}}{\lambda_{gc}} \right)} \qquad (8)$$

The length of the stub can be obtained as

$$l_s = \frac{\lambda_{g0}}{2\pi} arc \cot \left(m^2 B Z_s \right) - l_{s'} \qquad (9)$$

Similarly, the effective length of the short height-reduced waveguide is

$$l_m = \frac{\lambda_{gc}}{2\pi} \arcsin \frac{\omega_c C_p Z_0}{Y_m} \qquad (10)$$

In order to obtain the physical length of the short height-reduced waveguide, an extra length should be subtracted from the l_m according to the reference plane of the T-junction, as shown in Fig. 2. It is noted that the initial values of m, B, $l_{s'}$ and d_m are unknown because those values are closely related to the structure of the T-junction. In our design, the initial values are set to be $m = 1$, $B = 0$, $l'_s = 0$, and $d_m = 0$, respectively. After the dimensions of the filter are calculated by using (7)–(10), then the value of m, B, $l_{s'}$ and d_m can be obtained from [31] by using the calculated dimensions, effectively forming an iterative procedure. Employ the iterative procedure until the difference of the element values between two consecutive calculations is small enough, which results in the dimensions of the filter. After the initial dimensions of the filter are obtained, a fine tuning process can be carried out with CST Design Environment.

4. QUASI-ELLIPTIC WAVEGUIDE LOW-PASS FILTER

To verify the proposed design approach, an 11-order low-pass filter used for Ku-band satellite communications is designed and fabricated using a WR-75 waveguide. For this propose, the pass band and the stop band are chosen as 12.25–12.75 GHz and 14–14.5 GHz, respectively, which are typical frequency bands used in Asia. In order to maintain enough frequency deviation margin and to achieve high out-of-band attenuation, the cut-off frequency of the low-pass filter is chosen to be 13.3 GHz. The Chebyshev prototype used in the design is an 11-order low-pass filter with 0.05 dB ripple in the pass band. By impedance

and frequency scaling, the L-C values of the Chebyshev low-pass filter are calculated, as shown in Table 1. The attenuation poles are set in the stop band at $14.2\,$GHz, $14.3\,$GHz and $16\,$GHz, respectively. Accordingly, the elliptic low-pass filter net-work is obtained by using the method discussed above. The elliptic low-pass filter network is simulated and optimized by using Agilent ADS. The optimized L-C values are demonstrated in Table 2. As shown in Table 2, the maximum ratio of capacitances and inductances between the resonators is less than 2.8. In order to get a clear comparison, a standard elliptic low-pass filter network is designed by using Filter Design Guide module of Agilent ADS simulator. Its L-C values are also given in Table 2 for comparison. It can be seen from Table 2, the maximum ratio of capacitances between resonators in the standard elliptic low-pass filter net-work is over 12. Obviously, it is hard to realize them in the physical implementation. Fig. 7 shows the simulated responses of the Chebyshev low-pass filter network, proposed low-pass elliptic filter net-work and standard elliptic low-pass filter net-work, respectively. Simulated results are obtained using Agilent ADS. It is clearly shown that our proposed elliptic low-pass filter net-work has a sharp rejection performance and attenuation poles in the stop band, which is similar to the response of the standard elliptic low-pass filter network. As shown in Fig. 7, the return loss of the proposed elliptic filter network is more than $18\,$dB from $8.5\,$GHz to $13.3\,$GHz. Since the inductance elements in the Chebyshev low-pass filter are replaced by the parallel resonators, a little return loss deterioration in the lower pass band of the proposed elliptic filter network can be seen. However, the bandwidth of the pass band is enough for our application.

The initial physical dimensions of the filter are synthesized from the proposed L-C network by using the method discussed in the previous paragraph. Then, the filter is optimized by using CST Design Environment. Simulated results are shown in the Fig. 8, and compared to that of the proposed elliptic filter net-work. As shown in Fig. 8, they are in good agreement in the pass band and lower stop band of the filter. Transmission zeros are observed in both simulation results. Due to the coupling between the adjacent parallel resonators, the observed transmission zeros in the full wave simulation result have little deviation from that L-C network simulated result.

Table 1. L-C values of the Chebyshev low-pass filter net-work.

C_{pc1} (fF)	L_{sc2} (nH)	C_{pc3} (fF)	L_{s4} (nH)	C_{pc5} (fF)	L_{s6} (nH)	C_{pc7} (fF)	L_{sc8} (nH)	C_{pc9} (fF)	L_{sc10} (nH)	C_{pc11} (fF)
26.9	8.3	51.6	9.5	54.0	9.7	54.0	9.5	51.6	8.3	26.9

Table 2. *L-C* values of the elliptic low-pass filter net-work.

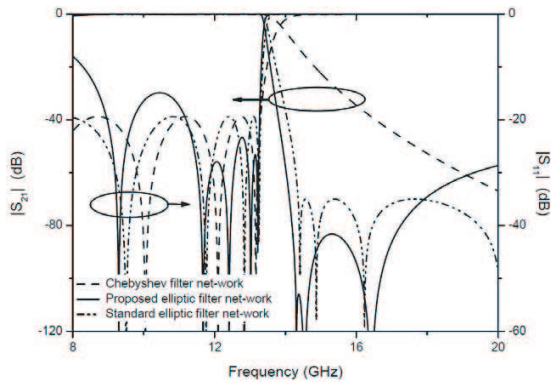| L-C parameter	C_{p1} (fF)	C_{s2} (fF)	L_{s2} (nH)	C_{p3} (fF)	C_{s4} (fF)	L_{s4} (nH)	C_{p5} (fF)	C_{s6} (fF)
Proposed	26.9	36.7	2.6	52.6	79.9	1.5	54.1	94.6
Standard	24.6	2.8	7.5	37.3	18.6	5.2	24.8	35.1
L-C parameter	L_{s6} (nH)	C_{p7} (fF)	C_{s8} (fF)	L_{s8} (nH)	C_{p9} (fF)	C_{s10} (fF)	L_{s10} (nH)	C_{p11} (fF)
Proposed	1.3	54.1	79.9	1.5	52.6	36.7	2.6	26.9
Standard	3.5	21.4	29.1	3.9	29.4	11.2	5.6	18.2

Figure 7. Simulated frequency response of the prototype net-works.
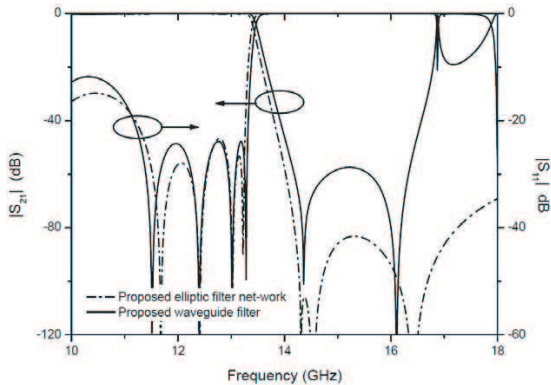

Figure 8. Comparison of the low-pass filter network and waveguide filter.

As the operating frequency increases, the impact of the higher-order modes in the waveguide, such as TE20 mode whose cut-off frequency is 15.74 GHz and TE11 mode of cut-off frequency 17.6 GHz, become significant, which cause the deterioration of the attenuation in the stop band and a second harmonic resonant frequency at 16.85 GHz, as shown in Fig. 8.

5. RESULTS AND DISCUSSIONS

Figure 9 shows simulated and measured results of the designed waveguide filter. It can be seen from measurements that the insertion loss is less than 0.3 dB and the return loss is more than 15 dB from 11 GHz to 13.5 GHz. The attenuation slope of the filter can be achieved up to 78 dB/GHz. The out-of-band rejection levels are larger than 39 dB from 14 GHz to 16 GHz. Obviously, the out-of-band rejection can be further improved with a lower cut-off frequency. As shown in Fig. 9, the measurements agree well with the simulations. The observed frequency deviation is believed to be caused by machining and assembly errors. A photograph of the fabricated low-pass filter is shown in Fig. 10. The size of it is $38 \, \text{mm} \times 38 \, \text{mm} \times 42 \, \text{mm}$, while the WR-75 flange size is $38 \, \text{mm} \times 38 \, \text{mm}$.

Due to the effect of higher-order modes in the waveguide, the proposed waveguide filter suffered a low second harmonic resonant frequency, as shown in Fig. 5, Fig. 8 and Fig. 9. As the cut-off frequencies of higher-order modes are dependent on the waveguide size, a smaller rectangular waveguide may be used to improve the stop band response of the filter.
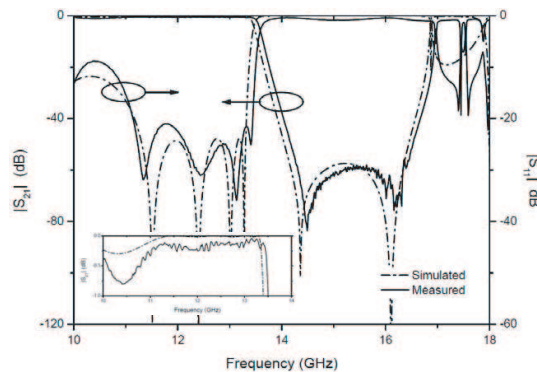

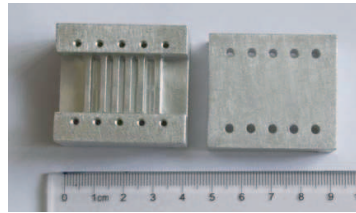**Figure 9.** Measured and simulated responses of the filter.

Figure 10. Photograph of the proposed low-pass filter.

6. CONCLUSION

A novel compact quasi-elliptic waveguide low-pass filter with very sharp out-of-band rejection for VSAT transceiver has been proposed in this paper. The equivalent model has been analyzed and the relevant parameters have been extracted. A quasi-elliptic low-pass prototype network, which is much easier in physical realization has also been proposed. Based on the equivalent model and proposed prototype network, a low-pass filter has been designed and tested, which is very small compared with traditional waveguide filters. Measured results have verified a low in-band insertion loss and a very sharp cut-off response. Moreover, the proposed quasi-elliptic low-pass prototype network may be used for designing other type filters.

REFERENCES

1. Maral, G., *VSAT Networks*, 2nd edition, Chapter 1, John Wiley & Sons, Inc., 2003.

2. Chen, H. and Y.-X. Zhang, "A novel and compact low-pass quasi-elliptic filter using hybrid microstrip/CPW structure," *Journal of Electromagnetic Waves and Applications*, Vol. 22, No. 17–18, 2347–2353, 2008.

3. Kuo, J.-T., S.-C. Tang, and S.-H. Lin, "Quasi-elliptic function bandpass filter with upper stopband extension and high rejection level using cross-coupled stepped-impedance resonators," *Progress In Electromagnetics Research*, Vol. 114, 395–405, 2011.

4. Yang, R.-Y., C.-M. Hsiung, C.-Y. Hung, and C.-C. Lin, "A high performance bandpass filter with a wide and deep stopband by using square stepped impedance resonators," *Journal of Electromagnetic Waves and Applications*, Vol. 24, No. 11–12, 1673–1683, 2010.

5. Paskiaraj, D., K.-J. Vinoy, and A.-T. Kalghatgi, "Analysis

and design of two layered ultra wide band filter," *Journal of Electromagnetic Waves and Applications*, Vol. 23, No. 8–9, 1235–1243, 2009.

6. AlHawari, A. R. H., A. Ismail, M. F. A. Rasid, R. S. A. R. Ab-dullah, B. K. Esfeh, and H. Adam, "Compact microstrip band-pass filter with sharp passband skirts using square spiral res-onators and embedded-resonators," *Journal of Electromagnetic Waves and Applications*, Vol. 23, No. 5–6, 675–683, 2009.

7. Shen, W., W.-Y, Yin, and X.-W. Sun, "Compact microstrip tri-section bandpass filters with mixed couplings," *Journal of Electromagnetic Waves and Applications*, Vol. 24, No. 13, 1807–1816, 2010.

8. Wang, Z., B. Zhao, Q. Lai, H. Zhong, R.-M. Xu, and W. Lin, "Design of novel millimeter-wave wideband bandpass filter based on three-line microstrip structure," *Journal of Electromagnetic Waves and Applications*, Vol. 24, No. 5–6, 671–680, 2010.

9. Zhu, Y.-Z., H.-S. Song, and K. Guan, "Design of optimized selective quasi-elliptic filters," *Journal of Electromagnetic Waves and Applications*, Vol. 23, No. 10, 1357–1366, 2009.

10. Zhou, J.-M., L.-H. Zhou, H. Tang, Y.-J. Yang, J.-X. Chen, and Z.-H. Bao, "Novel compact microstrip lowpass filters with wide stopband using defected ground structure," *Journal of Electromagnetic Waves and Applications*, Vol. 25, No. 7, 1009–1019, 2011.

11. Weng, L.-H., S.-J. Shi, X.-Q. Chen, Y.-C. Guo, and X. W. Shi, "A novel CSRRs DGS as lowpass filter," *Journal of Electromagnetic Waves and Applications*, Vol. 22, No. 14–15, 1899–1906, 2008.

12. Liu, H.-W., L.-Y. Li, X.-H. Li, and S.-X. Wang, "Compact microstrip lowpass filter using asymmetric stepped-impedance hairpin resonator and slotted ground plane," *Journal of Electromagnetic Waves and Applications*, Vol. 22, No. 11–12, 1615–1622, 2008.

13. Yu, W.-H., J.-C. Mou, X. Li, and X. Lv, "A compact filter with sharp-transition and wideband-rejection using the novel defected ground structure," *Journal of Electromagnetic Waves and Applications*, Vol. 23, No. 2–3, 329–340, 2009.

14. Xi, D., Y.-Z. Yin, L.-H. Wen, Y. Mo, and Y. Wang, "A compact low-pass filter with sharp cut-off and low insertion loss characteristic using novel defected ground structure," *Progress In Electromagnetics Research Letters*, Vol. 17, 133–143, 2010.

15. Mohra, A. S. S., "Compact lowpass filter with sharp transition band based on defected ground structures," *Progress In*

Electromagnetics Research Letters, Vol. 8, 83–92, 2009.

16. Sharp, E.-D., "A high-power, wide-band waffle-iron filter," *IEEE. Trans. Microw. Theory Tech.*, Vol. 11, No. 3, 111–116, 1963.

17. Lotfi Neyestanak, A.-A. and D. Oloumi, "Waveguide band pass filter with identical tapered posts," *Journal of Electromagnetic Waves and Applications*, Vol. 22, 2475–2484, 2008.

18. Levy, R., "Theory of direct-coupled-cavity filters," *IEEE Trans. Microw. Theory Tech.*, Vol. 15, No. 6, 340–348, 1967.

19. Levy, R., "Tappered corruagate waveguide low-pass filters," *IEEE Trans. Microw. Theory Tech.*, Vol. 21, No. 8, 526–532, 1973.

20. M.-H. Cheng and S.-M. Yang "Evanescent mode band reject filters and related methods (Patent Style)," U.S. Patent 5739734, Apr. 14, 1998.

21. Ghorbaninejad, H. and M.-K. Amirhosseini, "Compact bandpass filters utlilizing dielectric filled waveguides," *Progress In Electromagnetics Research B,* Vol. 7, 105–115, 2008.

22. Wang, R., L.-S. Wu, and X.-L. Zhou, "Compact folded substrate integrated waveguide cavities and bandpass filter," *Progress In Electromagnetics Research*, Vol. 84, 135–147, 2008.

23. Ismail, A., M.-S. Razalli, M.-A. Mahdi, R. S. A. Raja Abdullah, N. K. Noordin, and M. F. A. Rasid, "X-band trisection substrate-integrated waveguide quasi-elliptic filter," *Progress In Electromagnetics Research,* Vol. 85, 133–145, 2008.

24. Shen, W., W.-Y. Yin, X.-W. Sun, and J.-F. Mao, "Compact coplanar waveguide-incorporated substrate integrated waveguide (SIW) filter," *Journal of Electromagnetic Waves and Applications*, Vol. 24, No. 7, 871–879, 2010.

25. Shen, W., W.-Y. Yin, and X.-W. Sun, "Compact substrate integrated waveguide transversal filter with microstrip dual-mode resonator," *Journal of Electromagnetic Waves and Applications*, Vol. 24, No. 14–15, 1887–1896, 2010.

26. Li, R.-Q., X.-H. Tang, and F. Xiao, "Design of substrate integrated waveguide filters with source/load-multiresonator coupling," *Journal of Electromagnetic Waves and Applications*, Vol. 24, No. 14–15, 1967–1975, 2010.

27. Hu, G., C. Liu, L. Yan, K. Huang, and W. Menzel, "Novel dual mode substrate integrated waveguide band-pass filter," *Journal of Electromagnetic Waves and Applications*, Vol. 24, No. 11–12, 1661–1672, 2010.

28. Song, Q.-Y., H.-R. Cheng, X.-H. Wang, L. Xu, X.-Q. Chen, and X.-W. Shi, "Novel wideband bandpass filter integrating HMSIW

with DGS," *Journal of Electromagnetic Waves and Applications*, Vol. 23, No. 14–15, 2031–2040, 2009.

29. Wang, Z., Y. Jin, R. Xu, B. Yan, and W. Lin, "Substrate integrated folded waveguide (SIFW) partial H-plane filter with quarter wavelength resonators," *Journal of Electromagnetic Waves and Applications*, Vol. 24, No. 5–6, 607–617, 2010.

30. Levy, R. and I. Whitely, "Synthesis of distributed elliptic function filters from lumped-constant prototypes," *IEEE Trans. Microw. Theory Tech.*, Vol. 14, No. 11, 506–517, 1966.

31. Marcuvitz, N., *Waveguide Handbook*, The Institution of Electrical Engineering (IEE), London, UK, 1986.

32. Hong, J.-S. and M.-J. Lancaster, *Microstrip Filters for RF/Microwave Applications*, 44–46, John Wiley & Son, Inc., 2001.